RSC Mechanochemistry

ROYAL SOCIETY OF CHEMISTRY

PAPER

View Article Online
View Journal | View Issue

Cite this: *RSC Mechanochem.*, 2025, **2**, 297

Twin screw extrusion mechanochemical preparation of $BiVO_4$ hybrid pigments for coloring and reinforcing of acrylonitrile-butadiene-styrene†

Lei Wu,[a] Bin Mu,*[a] Hao Yang,[b] Zhaoli Wang,[c] Yongfeng Zhu,[a] Hui Dou[c] and Aiqin Wang*[a]

The traditional solid or liquid-phase preparation process of clay mineral-based inorganic pigments inevitably involves complex experimental procedures and generation of large volumes of polluting wastewater. To conform to the concept of green chemistry, a cleaner twin screw extrusion followed by high-temperature crystallization technology was developed to prepare low-cost $BiVO_4$ hybrid pigments based on a natural mixed-dimensional attapulgite clay (MDAPT). It was revealed that the generated shear and extrusion forces during the twin-screw extrusion process effectively promoted the formation of the precursor with the assistance of the colloidal properties of MDAPT. After incorporation of 60 wt% MDAPT, the hybrid pigments obtained at 700 °C presented the best color performance ($L^* = 74.76$, $a^* = 4.24$, $b^* = 80.84$). In view of the synergistic effect of each component, the hybrid pigments served as functional nanofillers for coloring and reinforcing of acrylonitrile-butadiene-styrene (ABS) after being modified with KH-570. At the optimum added amount of 2.75 wt% of hybrid pigments, the tensile strength and bending strength of yellow ABS composites increased by 36.87% and 25.96% compared with that of pure ABS, respectively. Furthermore, it was worth mentioning that incorporation of hybrid pigments also contributed to improving the UV-aging resistance of ABS due to the better absorption and reflection performances of hybrid pigments toward UV and visible light. Therefore, this study is expected to provide a feasible strategy for continuous mechanochemical preparation of low-cost $BiVO_4$ hybrid pigments for the coloring of ABS with excellent mechanical properties and aging-resistance.

Received 6th October 2024
Accepted 13th December 2024

DOI: 10.1039/d4mr00117f

rsc.li/RSCMechanochem

1. Introduction

Acrylonitrile-butadiene-styrene (ABS) is widely used for industry products, such as the structural components of automotive and consumer products, and the housing of pipes, electronic and electrical devices (machines, computers, telephones handsets, and televisions) by virtue of its easy processing, high surface gloss, good mechanical properties and chemical-resistance.[1–3] However, ABS polymers are vulnerable and age quickly when exposed to heating, oxygen or ultraviolet (UV) light. This is due to the C=C bonds in the butadiene component of ABS, which are easily broken under the conditions of UV radiation and oxygen, and ultimately means ABS polymers fail to meet performance requirements, subsequently limiting their further application.[4–6] Therefore, the aging of ABS polymers in outdoor applications has been a crucial issue hindering their implementation in end commercial products. To overcome this disadvantage and simultaneously enhance the mechanical properties of ABS products as well as endow them with a benign color, a feasible strategy has been recognized, in which various inorganic pigments are introduced as functional nanofillers with different colors into the polymer matrix.[7] Among the inorganic pigments, clay mineral-based inorganic hybrid pigments presented unique superiority in view of the synergistic effect of each component, especially the morphology, thermal stability, weather-resistance and low cost of clay minerals.[8,9]

In the case of the preparation routes of clay minerals-based inorganic hybrid pigments, the solid-phase (high-energy ball milling and vibratory milling)[10] and liquid-phase (chemical precipitation method, sol–gel method, hydrothermal or microwave-assisted hydrothermal method)[11–13] technologies are still the mainstream synthesis methods. It has been confirmed that incorporation of clay minerals obviously reduced the pigment production cost and improved the color properties of inorganic pigments due to the doping of chemical compositions of clay minerals and the control of the particle size and

[a]Key Laboratory of Clay Minerals of Gansu Province, Research Center of Resource Chemistry and Energy Materials, Lanzhou Institute of Chemical Physics, Chinese Academy of Sciences, Lanzhou 730000, China. E-mail: mubin@licp.cas.cn; aqwang@licp.cas.cn

[b]Shenzhen Key Laboratory of Interfacial Science and Engineering of Materials, Department of Materials Science and Engineering, Southern University of Science and Technology, Shenzhen 518055, China

[c]Gansu Road & Bridge Construction Group, Lanzhou 730000, China

† Electronic supplementary information (ESI) available. See DOI: https://doi.org/10.1039/d4mr00117f

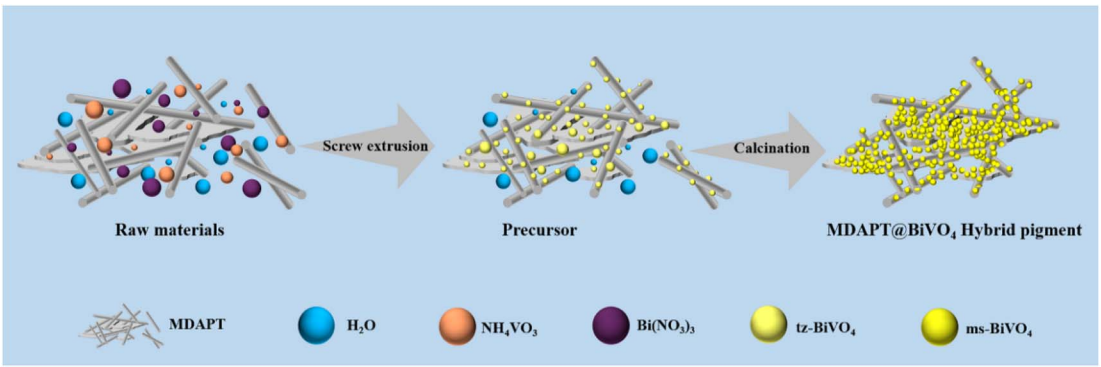

Fig. 1 A schematic diagram of the preparation process of $BiVO_4$ hybrid pigments.

dispersion of the pigment particles. Although the solid-phase experimental processes exhibited obvious advantages due to fewer steps and shorter process flow for the preparation of the clay minerals-based inorganic hybrid pigments, the defects of the intermittent preparation mode and high energy consumption are increasingly evident with the swift development of science and technology. Compared with the solid-phase route, the liquid-phase method presented obvious advantages for controlling the purity, size and color of clay mineral-based inorganic hybrid pigments. However, it inevitably involves discharge of large volumes of wastewater and organic solvents. To conform with the principles of green chemistry, it is urgently required to develop cleaner production technology with little or no waste discharge for the preparation of high-performance clay minerals-based inorganic hybrid pigments.

Different from the common solid-phase and liquid-phase preparation routes, twin screw extrusion is an emerging and popular technology in the fields of chemistry and material science, which uses minimal solvent or no solvent to synthesize new compounds and materials by continuous mixing or the chemical reaction of reactants under shearing and kneading forces.[14] Therefore, twin screw extrusion could be an alternative strategy for replacing liquid-phase methods to fabricate clay mineral-based inorganic hybrid pigments, and it is of great significance to investigate the feasibility of preparing clay minerals-based inorganic hybrid pigments by twin screw extrusion technology, which can not only conform to the principles of green chemistry, but also provide a clean solvent-free scheme for the preparation of clay minerals-based inorganic hybrid pigment on an industrial scale.

China is one of the main countries possessing abundant reserves of attapulgite (APT) clay in the world.[15,16] However, the APT clay resource in Gansu province has more complex associated ores with one-dimensional and two-dimensional mixed morphologies as well as a deeper red color due to the formation cause of lacustrine deposits, and has been named as mix-dimensional APT clay (MDAPT). It was reported that the color of MDAPT mainly resulted from hematite and isomorphism substitution of iron ions (Fe^{2+} and Fe^{3+}) with octahedral Mg^{2+} or Al^{3+}. In order to realize the large-scale applications of raw MDAPT in related industrial fields and high-quality development of the MDAPT industry, this study employed twin screw extrusion for the cleaner preparation of MDAPT-based $BiVO_4$ (MDAPT@$BiVO_4$) hybrid pigments for coloring and reinforcing of ABS using MDAPT, bismuth nitrate hydrate, and ammonium meta-vanadate as the raw materials (Fig. 1), in which $BiVO_4$ hybrid pigments were modified with 3-methacryloxy-propyltrimet-hoxysilane (KH-570) to improve the surface/interfacial compatibility between hybrid pigments and ABS matrix. The effects of hybrid pigment content on the coloring, thermal, mechanical and ageing properties of ABS composites were comparatively studied in detail compared with the pure ABS. In addition, the possible structure–activity relationship was analyzed and discussed.

2. Experimental

2.1 Materials

The raw MDAPT originated from the Dimaitong Mine, Gansu Province, China. Oxalic acid dihydrate (OA, $C_2H_2O_4 \cdot 2H_2O$, AR) was purchased from Sichuan Xilong Chemical Co., Ltd (Sichuan, China). KH-570 was obtained from Nanjing United Silicon Chemical Co., Ltd (Nanjing, China). Ethanol was gained from Tianjin Langmaoshiye Industrial Co., Ltd. Bismuth nitrate hydrate ($Bi(NO_3)_3 \cdot 5H_2O$, AR) and ammonium meta-vanadate (NH_4VO_3, AR) were purchased by Chengdu Kelong Chemical Industry Co., Ltd (Chengdu, China), while ABS was provided by KUMHO-SUNNY Plastics Co., Ltd. Other reagents were all analytical grade and used without further purification.

2.2 Preparation of the precursors of MDAPT@$BiVO_4$ hybrid pigments

Typically, the raw MDAPT was firstly treated with 1 mol L^{-1} OA for 10 h at a solid-to-liquid ratio of 1 : 20, 90 °C and 400 rpm to remove the main color-causing ions (*e.g.*, Fe^{3+}), and then the solid product was centrifugated, washed three times with water, dried at 60 °C, ground and passed through a 400-mesh sieve before use. Next, 35.67 g of $Bi(NO_3)_3 \cdot 5H_2O$, 22.587 g of NH_4VO_3 and 24 g of MDAPT (60 wt% of theoretical yield of $BiVO_4$) were well mixed in a beaker, and then the premixed samples were put in the extruder and extruded for 10 times (FT-26 twin-screw extruder, Guangzhou Huagong Optical Mechanical & Electrical

Technology Co. Ltd) with the working parameters including screw speeds of 80 rpm and extruder pressure of 5 kg at room temperature. Then a series of precursors of MDAPT@$BiVO_4$ hybrid pigments containing different weight fractions of MDAPT (20 wt%, 40 wt%, 60 wt% and 80 wt%) were prepared and abbreviated as pre-MDAPT@$BiVO_4$.

2.3 Preparation of MDAPT@$BiVO_4$ hybrid pigments

The calcining of the precursors in a muffle furnace was conducted at different temperatures for 120 min with a heating rate of 10 °C min^{-1} from room temperature to prepare MDAPT@$BiVO_4$ hybrid pigments. The effects of calcination temperature (300 °C, 400 °C, 500 °C, 600 °C, 700 °C and 800 °C) and addition amount of MDAPT (20 wt%, 40 wt%, 60 wt% and 80 wt%) on the color performance of the pigments were systematically investigated. The prepared composite pigments were labelled as MDAPT@$BiVO_4$-*T*-*M*, where *T* represented the calcining temperature, while *M* was the addition amount of MDAPT. As a control, the hybrid pigments were also prepared after incorporation of 60 wt% raw MDAPT by the same procedures, and the product was marked as RMDAPT@$BiVO_4$-*T*-60, where *T* represented the calcining temperature.

2.4 Surface modification of BVO_4 hybrid pigments

Firstly, 3.0 g of MDAPT@$BiVO_4$ hybrid pigments was well dispersed in 30 mL absolute ethanol under sonication. Next, 7 wt% of KH-570 was dissolved in the above dispersion to form a light-yellow solution. Then the prepared solution was heated at 80 °C for 12 h. After being cooled to room temperature, the solid sample was collected by centrifugation and washed with deionized water and ethanol several times, and the product was obtained after being dried at 60 °C for 24 h. Finally, the dry solid product was ground and passed through a 400-mesh sieve for further use.

2.5 Evaluation of chemical stability

The chemical stability of the hybrid pigments was evaluated using 1 mol L^{-1} HCl solution, 1 mol L^{-1} NaOH solution and anhydrous ethanol. Typically, 2.0 g of hybrid pigments was immersed in 15 mL of the aforementioned solutions or solvents and stirred at room temperature for 24 h. After being immersed, centrifuged, dried in an oven at 60 °C, the color coordinates of hybrid pigment were measured by comparing the color coordinates of hybrid pigments before and after immersion.

2.6 Preparation of the colorful ABS composite

The prepared hybrid pigments and ABS granules were firstly dried at 80 °C for 12 h before being mixed with each other, then the polymer composites were obtained after melt mixing of ABS granules and hybrid pigments in a single screw extruder. To reach a better distribution and dispersion of hybrid pigments throughout the ABS matrix, all the mixtures were extruded twice using the single screw extrude with the working parameter of extruder temperature of 200 °C and rotation speed of 80 rpm. The standard tensile spline model and curved spline model was prepared by putting the above polymer composites into the injection molding machine with the extrusion temperature of 200 °C and moulding temperature of 40 °C. The content of hybrid pigments in the ABS matrix was 0.25 wt%, 0.50 wt%, 0.75 wt%, 1.00 wt%, 1.25 wt%, 1.50 wt%, 1.75 wt%, 2.00 wt%, 2.50 wt%, 2.75 wt% and 3.00 wt%, respectively.

2.7 Mechanical properties test of ABS composites

All the mechanical properties tests of the tensile splines and curved spline were performed on a universal testing machine (SANS general material testing instrument, CMT4304) at room temperature with a load cell of 1000 N and test speed of 3 mm min^{-1}. The initial gauge length of tensile splines is 30 mm and the curved spline is 64 mm. Each series of tensile splines and curved spline was tested in parallel at least five times and the averages were reported.

2.8 Evaluation of the anti-aging performance

The accelerated aging experiment was conducted by exposing the polymer composites to a fluorescent UV lamp (lamp 2 A, 40 W, UV A-313) for 120 h at the black panel 60 °C in the UV aging chamber (Xinlang electronic, ZN-P). The samples were taken out every 24 h to conduct the UV ageing test, and each series of samples were tested in parallel five times and the averages were reported.

2.9 Characterizations

The commission International de l'Eclairage (CIE)-$L^*a^*b^*$ colorimetric method was used to characterize the color values of the as-prepared pigments on a Color-Eye automatic differential colorimeter (X-Rite, Ci 7800, USA), where L^* is the lightness axis (0 for black and 100 for white), a^* is the green-red axis (negative for green and positive for red) and b^* is the blue-yellow axis (negative for blue and positive for yellow). Fourier transform infrared (FTIR) spectra of hybrid pigments samples were collected on a Nicolet NEXUS FTIR spectrometer (Thermo Nicolet 6700, Thermo Fisher, USA) in the wavenumber range of 4000–400 cm^{-1} using KBr tabletting method. XRD patterns were collected in the range of 3° to 80° (2θ) at a scanning rate of 0.05° s^{-1} with a step interval of about 0.167° at room temperature on a SmartLab SE multifunctional X-ray diffractometer (Rigaku Co., Japan), equipped with a Cu-Kα radiation source (λ = 1.540598 Å, 40 kV, 40 mA). The micro-morphology of the hybrid pigments sample was observed on a JEM-2100 transmission electron microscope (TEM, Field Electron and Ion Co., USA) after being dispersed into ethanol and kept in an ultrasonic bath for 20 min. The dispersion of hybrid pigments in ABS matrix and the fracture surface morphology of ABS composites after the tensile tests were observed using a JSM-6701F scanning electron microscopy (JEOL, Ltd Japan), the ABS splines were treated by freezing in liquid nitrogen first before observing. Energy dispersive X-ray spectroscopy (EDX, JSM-5600LV, Japanese Electronic Optical Co., Ltd, Japan) was used to determine the composition and distribution of surface element of the as-prepared samples. Similarly, pure ABS splines were also

treated by freezing in liquid nitrogen to obtain a ruptured surface.

3. Results and discussion

3.1 Preparation condition optimization of hybrid pigments

Fig. 2a–d depicts the color parameters of $BiVO_4$ hybrid pigments prepared at different calcining temperatures and different amounts of MDAPT added. As the calcining temperature decreased below 800 °C, the brightness value (L^*), redness value (a^*) and yellowness value (b^*) of MDAPT@$BiVO_4$ hybrid pigments increasingly improved (Fig. 2e). However, the color parameters began to decrease when the calcining temperature reached 800 °C, which might be caused by the coating of $BiVO_4$ on the MDAPT surface, the damage of crystal structure of MDAPT and the nanochannel collapse of APT at high temperature with the removal of zeolitic water, structural water and the de-hydroxylation. In addition, hybrid pigments possessed the maximum b^* value when the calcining temperature was up to 700 °C. At the optimum calcining temperature, the prepared $BiVO_4$ pigments exhibited better color performance when the added amount of MDAPT was relatively low (20–60 wt%). By contrast, MDAPT@$BiVO_4$ hybrid pigments presented the optimal color performance when the added amount of MDAPT was 60 wt% ($L^* = 74.76$, $a^* = 4.24$ and $b^* = 80.84$). It suggested that the low added amount of MDAPT did not contribute to the benign dispersion of $BiVO_4$ particles on the surface of MDAPT, while the high incorporation amount of MDAPT (80 wt%) resulted in the presence of MDAPT agglomeration. Based on the above analysis, the optimum preparation conditions were summarized as follows: calcination temperature was 700 °C and added amount of MDAPT was 60 wt%.

Furthermore, pure $BiVO_4$ and hybrid pigments prepared with raw MDAPT as the carrier were also prepared using the same process (Fig. S1†). After calcination treatment above 500 °C, the color of pure $BiVO_4$ changed significantly, as shown in

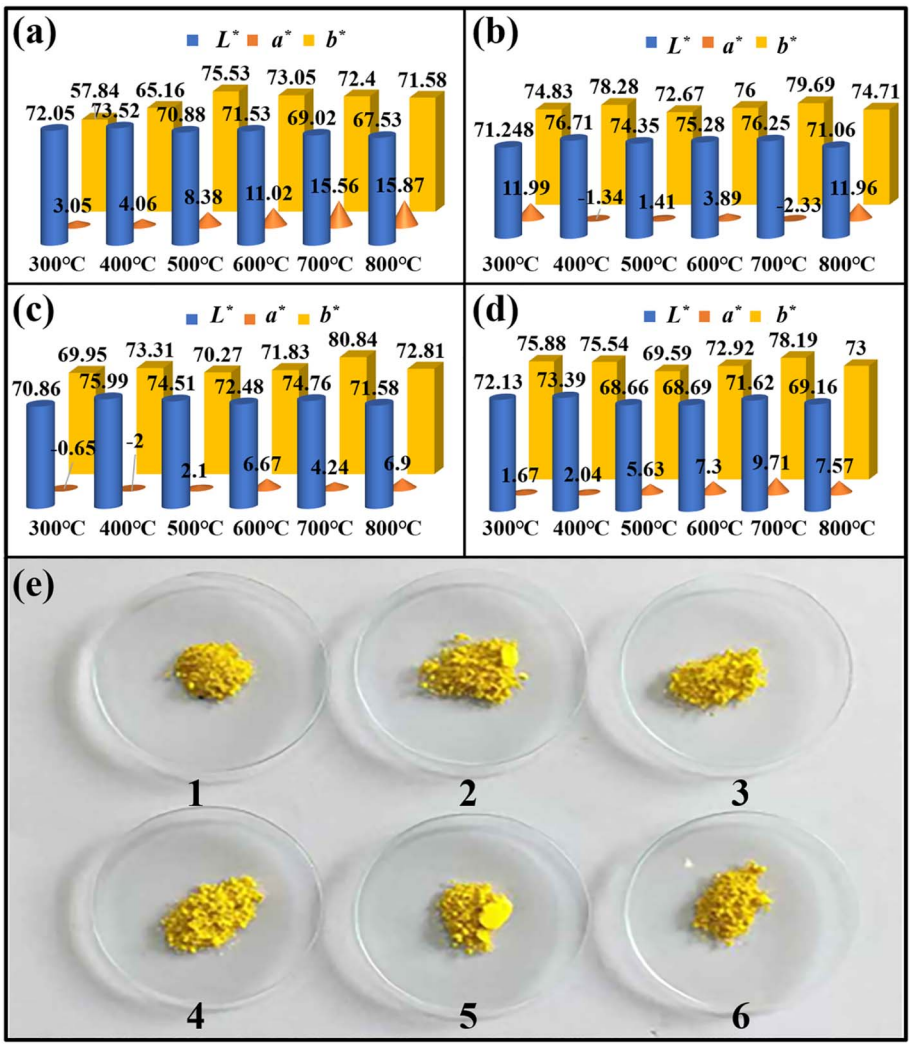

Fig. 2 Color coordinates of MDAPT@$BiVO_4$ hybrid pigments prepared with different amounts of MDAPT and different calcining temperatures: (a) 20 wt%, (b) 40 wt%, (c) 60 wt%, and (d) 80 wt%). (e) Digital photographs of the hybrid pigments prepared at different calcining temperatures after incorporation of 60 wt% MDAPT.

Fig. S1a.† The L^* and b^* values of the pigments decreased from 67.39 and 72.48 to 59.97 and 51.8, respectively. Compared with the hybrid pigment prepared using OA leached MDAPT, the color parameters of the hybrid pigment prepared based on raw MDAPT decreased significantly with a high red value, and low brightness and yellow values at the same calcination temperature, as shown in Fig. S1b.† This suggested that the introduction of MDAPT improved the color performance of $BiVO_4$, especially OA leached MDAPT.

The crystal phase composition of MDAPT and MDAPT@$BiVO_4$-*T*-60 hybrid pigments were studied by XRD patterns (Fig. 3a). In the case of raw MDAPT, the diffraction peaks at $2\theta = 8.48°$, 19.81°, and 34.94° were attributed to APT, corresponding to (110), (040) and (400) planes, respectively. The peaks of quartz were observed at $2\theta = 20.88°$ (100), 26.7° (101), 36.55° (110), 42.45° (200), 50.13° (112), 59.94° (211) and 68.14° (203), respectively. In addition, the peaks at $2\theta = 8.836°$ were assigned to illite.[17] Therefore, the main crystalline phases of MDAPT were composed of APT, quartz and illite. After incorporation of $BiVO_4$, the characteristic diffraction peaks of monoclonal scheelite type $BiVO_4$ (ms-$BiVO_4$) appeared at $2\theta =$ 18.98°, 28.58°, 30.54°, 34.49°, 35.22°, 39.78°, 42.46°, 45.88°, 46.71°, 47.30°, 50.31°, 53.44°, 56.06°, 58.53° and 59.26°, which were assigned to (011), (−130), (040), (200), (002), (211), (051), (−132), (210), (042), (202), (310), (−152), (321) and (123) planes,[18] respectively, suggesting the successful formation of ms-$BiVO_4$. However, the characteristic peaks of the main crystal phases of MDAPT vanished, while the diffraction peaks of APT were very weak after incorporating of $BiVO_4$ at above 600 °C (Fig. 3a). This phenomenon might be due to the decrease in the content of MDAPT with the introduction of $BiVO_4$ and the damage of crystal structure of clay minerals at high temperature.

FTIR spectra of MDAPT@$BiVO_4$-*T*-60 were further used to confirm the presence of $BiVO_4$ in the hybrid pigments. As shown in Fig. 3b, the characteristic absorption bands of the stretching vibrations of hydroxyl groups (Al–OH and Si–OH), Si–O–Si, and the physically adsorbed water were found at 3414–3730 cm^{-1}, 1029–1065 cm^{-1} and 1625–1634 cm^{-1}, respectively.[19,20] The band at 531–534 cm^{-1} was attributed to the Si–O–Al stretching vibration. In the case of $BiVO_4$, the main absorption bands were almost the same before and after annealing. The symmetric and asymmetric stretching/bending vibrations of V–O bond in VO_4^{3-} and the weak and intense stretching and bending vibrations of Bi–O were observed near 720–729 cm^{-1}, 824 cm^{-1} and 472–475 cm^{-1}, respectively.[21,22] In addition, it was worth noting that the characteristic peaks of the Si–O–Al bond were very weak or even disappeared after incorporating $BiVO_4$ at different temperatures, and the positions of the $BiVO_4$ diffraction peaks presented an obvious shift after incorporation of MDAPT and the calcining process, which might be due to the collapse of the nanochannel of APT and high crystallinity of $BiVO_4$. To improve the dispersion of MDAPT@$BiVO_4$-700-60 hybrid pigments in the ABS matrix, hybrid pigments were modified with KH-570. As shown in Fig. S2,† the absorption bands at 2932 cm^{-1} and 2851 cm^{-1} corresponded to the C–H stretching vibration peaks of $-CH_2$ and $-CH_3$ of KH-570, respectively, indicating that MDAPT@$BiVO_4$-700-60 hybrid pigments were successfully modified with KH-570.

Fig. 4 depicts the TEM images of MDAPT before and after OA treatment. As shown in Fig. 4a, MDAPT was mainly composed of one-dimensional nanorods and two-dimensional nanoflakes. Combined with XRD analysis, the lamellar morphology was mainly ascribed to illite, while APT possessed a typical rod-like morphology but there was severe agglomeration among the nanorods. After OA treatment, the rod-like morphology and length of nanorods were maintained, but the number of

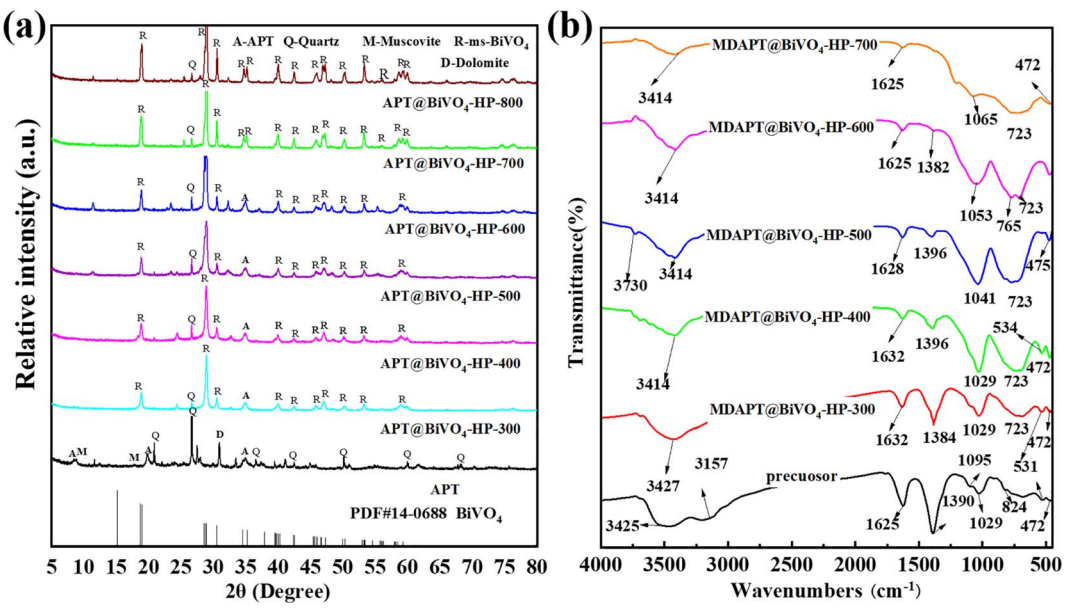

Fig. 3 XRD patterns (a) and FTIR spectra (b) of hybrid pigments prepared at different calcination temperatures after introduction of 60 wt% MDAPT.

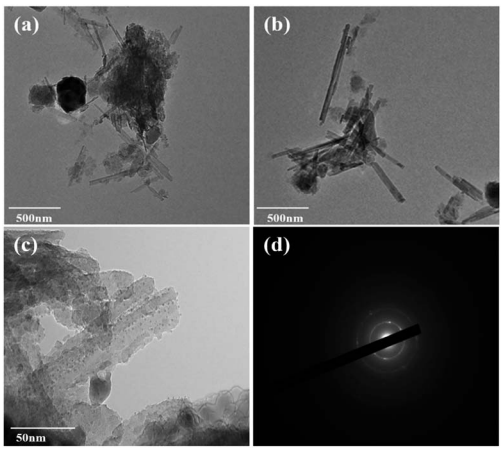

Fig. 4 TEM images of before (a) and after (b) oxalic acid treatment of MDAPT, (c) TEM and (d) electron diffraction images of MDAPT @$BiVO_4$-700-60.

nanorod bundles or agglomerates decreased (Fig. 4b), indicating that OA treatment enhanced the dispersion of nanorods with the removal of the impurities. After introducing $BiVO_4$ nanoparticles, it was evident that the $BiVO_4$ nanoparticles were uniformly anchored on the surface of the one-dimensional and two-dimensional matrix (Fig. 4c), rendering the surface of MDAPT rougher. By contrast, severe aggregation of the rod-like structure emerged due to the sintering of hybrid pigments. Furthermore, the SAED image also indicated that $BiVO_4$ prepared at 700 °C was single crystalline (Fig. 4d).

3.2 Coloring properties

Fig. 5a shows the digital photos of RMDAPT@$BiVO_4$-700-60, MDAPT@$BiVO_4$-700-60, and KH-570 modified MDAPT@$BiVO_4$-700-60. It was found that the hybrid pigment prepared using raw MDAPT was orange, while it was yellow fabricated based on OA leached MDAPT. In fact, the color of the yellow pigments in the color space $L^*a^*b^*$ (CIELAB system) was mainly related to the b^* value, and the yellow hue of the hybrid pigments exhibited a positive relation with the positive b^* value. As shown in Fig. 5b, hybrid pigments prepared by raw MDAPT exhibited a low b^* value and high a^* value, while hybrid pigment based on OA-treated MDAPT presented a high b^* value and low a^* value. This might be due to the removal of the free hematite and color-causing ions from MDAPT by OA. Compared with the red color of the raw MDAPT, OA-treated MDAPT was white (Fig. S3†), indicating that the color-causing impurities were dissolved by OA. Generally, OA dissolved metal ions by breaking the Si–O–M bond, and the ability to coordinate with metal ions might accelerate the dissolution of metal ions. The chemical composition of MDAPT before and after OA treatment was shown in Table S1.† After being treated with OA, the contents of Fe_2O_3, MgO, Al_2O_3 and Na_2O of MDAPT decreased from 4.49% to 2.54%, 5.31% to 1.84%, 13.18% to 11.51% and 1.11% to 0.42%, respectively, which might reduce the negative effect of color-causing ions on the color properties of hybrid pigments. By contrast, the color of MDAPT@$BiVO_4$-700-60 underwent a slight change after being modified with KH-570 ($L^* = 75.48$, $a^* = 1.09$, $b^* = 83.04$), which could be due to the change of the absorbance and reflection of hybrid pigments to visible light before and after decoration with KH-570. In addition, it was found that the reflection of visible light of the as-prepared MDAPT@$BiVO_4$-700-60 above 400 nm was increased compared with the raw MDAPT@$BiVO_4$-700-60 according to the UV-vis diffuse reflectance spectra (Fig. S4†), which also confirmed that the prepared MDAPT@$BiVO_4$-700-60 presented a better color performance than that of RMDAPT@$BiVO_4$-700-60.

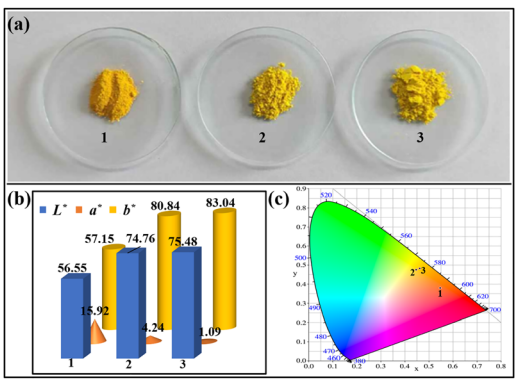

Fig. 5 (a) Digital photographs of the prepared hybrid pigments, the chromaticity values of (b) the pigments and (c) chromaticity CIE coordinate diagram ((1) Raw MDAPT@$BiVO_4$-700-60, (2) MDAPT@$BiVO_4$-700-60, (3) KH-570 modified MDAPT@$BiVO_4$-700-60).

3.3 Evaluation of chemical stability

As summarized in Fig. S5,† there was no obvious color variation that the naked eye could distinguish after HCl, NaOH and ethanol treatment compared with the original MDAPT@$BiVO_4$-700-60 hybrid pigments. Moreover, the color saturation hardly changed before and after different treatments. From Table S2,† no obvious changes were observed from the color parameters of the samples treated with HCl or NaOH solution compared with that of the original MDAPT@$BiVO_4$-700-60, suggesting the prepared pigments presented benign acid and alkali resistance. Although there was a slight decrease in the brightness (L^*) after treatment by ethanol, the high b^* value could still satisfy the requirements of the related application fields to the yellowness values (Table S2†). Thus, the minor color value changes indicated that the as-prepared hybrid pigments possessed good environmental stability.

After being modified with KH-570, MDAPT@$BiVO_4$-700-60 was incorporated into the ABS matrix to obtain yellow ABS composites (Fig. 6). Obviously, the greater the amounts of hybrid pigments added, the deeper the color of the ABS composites, which could be attributed to the fact that KH-570 modification improved the surface/interfacial compatibility between hybrid pigments and the ABS matrix, significantly enhancing their dispersion in the ABS matrix. No obvious difference in the color variation was observed for the ABS composites spline when the added amount of KH-570 modified MDAPT@$BiVO_4$-700-60 was higher than 1.5 wt%. This phenomenon was also consistent with

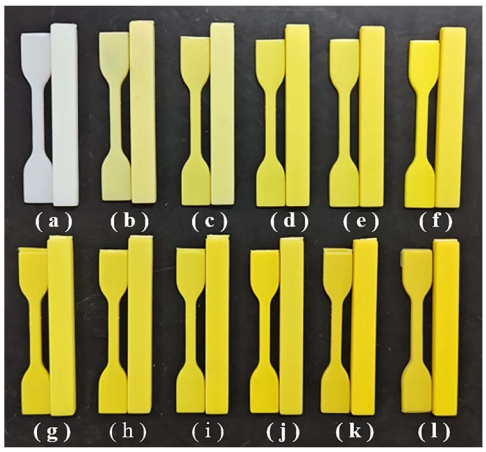

Fig. 6 Tensile and bending splines of ABS composites containing different contents of KH-570 modified MDAPT@$BiVO_4$-700-60 ((a): 0.00 wt%, (b): 0.25 wt%, (c): 0.50 wt%, (d): 0.75 wt%, (e): 1.00 wt%, (f): 1.25 wt%, (g): 1.50 wt%, (h): 1.75 wt%, (i): 2.00 wt%, (j): 2.50 wt%, (k): 2.75 wt%, and (l): 3.00 wt%).

Table 1 Chromatic values of ABS composites containing different contents of KH-570 modified MDAPT@$BiVO_4$-700-60

	Color parameters of ABS composites					
Pigment content	L^*	a^*	b^*	C^*	h^*	ASTM E313
0.00 wt%	58.09	−6.15	−7.83	9.96	231.85	−8.65
0.25 wt%	61.97	−11.67	32.09	34.15	109.98	56.53
0.50 wt%	62.29	−14.85	35.02	38.04	112.97	57.69
0.75 wt%	61.98	−14.58	35.43	38.31	112.37	58.73
1.00 wt%	69.51	−13.74	67.18	68.57	101.56	90.19
1.25 wt%	70.56	−13.10	68.25	69.50	100.87	91.11
1.50 wt%	68.65	−14.30	65.87	67.40	102.25	84.98
1.75 wt%	68.11	−10.94	66.76	67.65	99.31	93.15
2.00 wt%	73.31	−11.92	74.51	75.46	99.09	95.30
2.50 wt%	72.11	−13.15	73.36	74.53	100.17	93.94
2.75 wt%	71.66	−12.59	76.38	77.41	99.36	96.52
3.00 wt%	71.81	−12.42	75.92	76.93	99.29	96.34

the CIE $L^*a^*b^*$ color parameters (Table 1). Compared with pure ABS ($L^* = 58.09$, $a^* = -6.15$, $b^* = -7.83$), the L^* and b^* values of the ABS composites decreased initially and subsequently increased, and the a^* values increased initially and subsequently decreased with the increase in the added amount of KH-570 modified MDAPT@$BiVO_4$-700-60. Specifically, the b^* value of the ABS composites reached 65.25 after incorporation of 1.25 wt% KH-570 modified MDAPT@$BiVO_4$-700-60-HP, and the ABS composite presented the best color performance ($L^* = 71.66$, $a^* = -12.59$, $b^* = 76.38$) as the added amount of hybrid pigments was 2.75 wt%, and then it slightly decreased ($L^* = 71.81$, $a^* = -12.42$, $b^* = 75.92$) at the added amount of 3.00 wt%. This phenomenon could be attributed to the presence of the aggregation phenomenon of the introduced excessive pigment particles.[23] Thus, the optimum added amount of KH-570 modified MDAPT@$BiVO_4$-700-60 was determined as 2.75 wt%.

3.4 Mechanical properties of ABS composites

Fig. 7a–c shows the mechanical properties of pure ABS and ABS composites, which were characterized by the tensile strength testing and bending strength testing. The tensile strength, elongation at break and bending strength of pure ABS were 45.25 MPa, 13.06% and 75.35 MPa, respectively. Compared with the mechanical properties of pure ABS, the tensile strength of ABS composites was obviously improved with the increase in the added amount of KH-570 modified MDAPT@$BiVO_4$-700-60, and it reached a maximum when the added amount was 2.75 wt%, and the tensile strength and bending strength of ABS composites increased by 36.87% and 25.96%, respectively. However, the mechanical properties of the ABS composites began to decrease when the content of hybrid pigments was more than 2.75 wt%. In fact, the increase in the tensile strength and bending strength of ABS composites depended on the surface/interfacial compatibility between the hybrid pigments and ABS matrix.[24,25] The decrease in the mechanical properties of ABS composites could be related to the aggregation phenomenon of excessive pigment particles in the ABS matrix.[26,27] In order to achieve a desirable balance between reinforcement and toughness, the optimum content of KH-570 modified MDAPT @$BiVO_4$-700-60 was determined to be 2.75 wt%, taking into account the comprehensive mechanical properties of the ABS composites.

Fig. 7d and e illustrate the SEM images of the tensile failure section of ABS and ABS composites. It was observed that the section of pure ABS existed in the form of water waves (Fig. 7d). Compared with the SEM images of pure ABS, ABS composites containing modified pigment presented a plain and compact surface, which could be attributed to the good dispersion of MDAPT@$BiVO_4$-700-60 in ABS matrix. It suggested that KH-570 modification realized a surface adjustment of hybrid pigments from hydrophilic to hydrophobic, which increased the surface/interfacial compatibility between pigments particles and the ABS matrix. In addition, the thermal degradation of ABS and ABS composites was investigated under nitrogen atmosphere at the same temperature (Fig. 7f). Below 300 °C, there was almost no obvious mass loss for both pure ABS and ABS composites. With the increase in the temperature, the sharp mass losses for all of samples were observed, which was related to the thermal degradation of ABS. The thermal degradation of ABS consisted of two stages, the first step initiated at 200 °C and ended at 400 °C, while the decomposition of butadiene started at 340 °C and styrene at 350 °C. The second step ranged from 400 until 550 °C, which involved the decomposition of acrylonitrile beginning at 400 °C. Due to the low added amount of hybrid pigments, incorporation of hybrid pigments hardly affected the thermal degradation of ABS, but ABS composites exhibited a higher thermal decomposition temperature and lower mass loss than pure ABS at the same heating temperature. This phenomenon could be attributed to the synergistic effect of each component in hybrid pigments. On the one hand, the removal of the physically adsorbed water and zeolitic water in MDAPT could hinder the thermal degradation of ABS during the heating process. On the other hand, the surface/interface compatibility

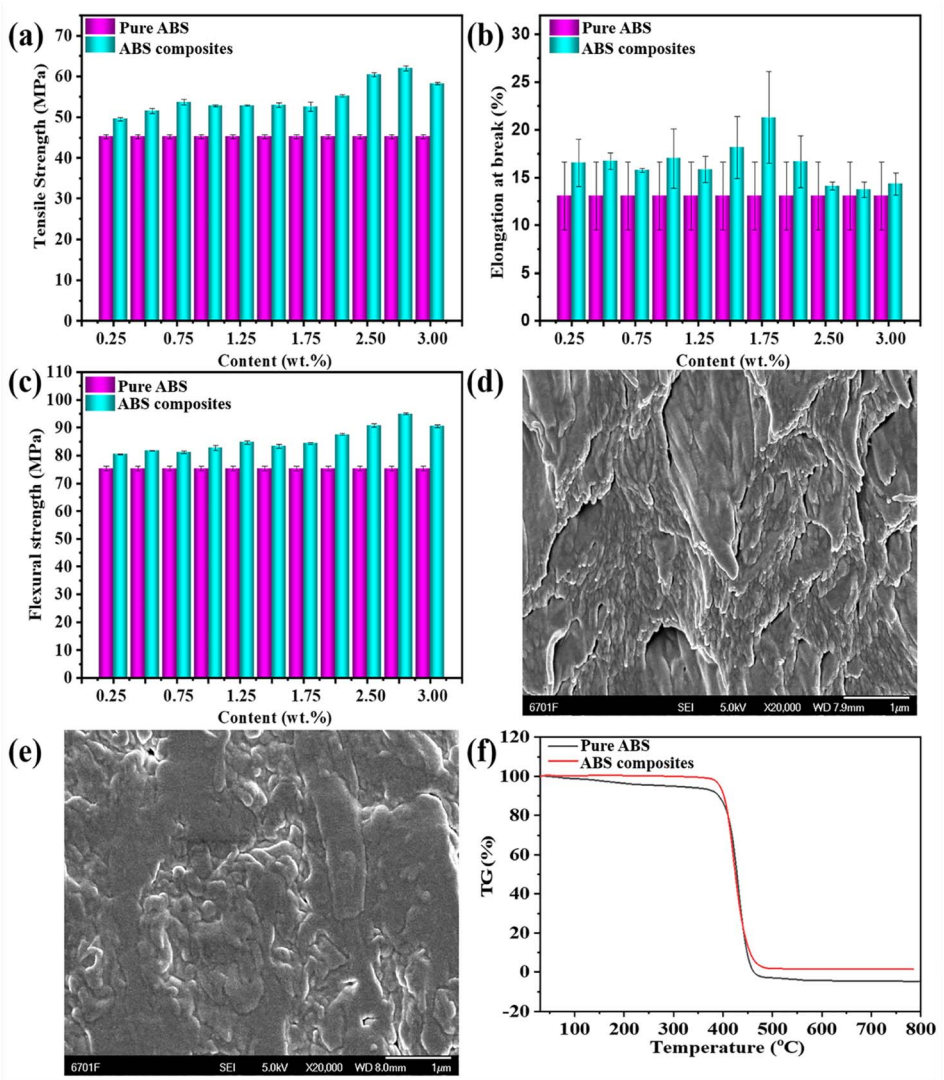

Fig. 7 Effect of the contents of hybrid pigments on the mechanical properties of ABS composites: (a) tensile strength, (b) elongation at break and (c) bending strength. SEM images of the bending failure section for (d) pure ABS and (e) ABS composites, (f) TGA curves of pure ABS and ABS composites.

and interfacial bonding between hybrid pigments and ABS were enhanced after being modified with KH570 accompanied with the good dispersion of hybrid pigments in ABS matrix, which effectively prevented gas out-diffusion derived from the degraded product and shielded the penetration of free radicals generated during thermal decomposition, resulting in the inhibition of the thermal degradation of ABS.[28–30] Due to the incorporated amount of MDAPT@$BiVO_4$-700-60 in ABS being small, ABS and ABS composites almost presented the same maximum decomposition temperature. Consequently, incorporation of MDAPT@$BiVO_4$-700-60 also endowed the ABS with benign thermal stability on the basis of coloring and reinforcing performances.

In addition, the element mappings are used to probe the dispersion of the incorporated hybrid pigments in the ABS matrix. As depicted in Fig. 8, the C and N elements were found in the elemental mapping images of pure ABS, which was also consistent with the chemical compositions of ABS. After incorporation of KH570 modified MDAPT@$BiVO_4$-700-60, the elements of O, Bi, V, Al, Mg and Fe were observed besides C and N, and all of elements were uniformly distributed in the ABS composites. In other words, the modified MDAPT@$BiVO_4$-700-60-HP presented good dispersion in the ABS matrix.

3.5 Aging-resistance of ABS composites

It is well-known that the ABS is widely used for tough products, because of its property–price profile intermediates between inexpensive thermoplastic and high-performance engineering plastics.[31,32] However, one critical drawback of ABS is its poor UV-resistance, which is caused by the existing butadiene component. When ABS is used in outdoor applications, the C=C bonds in butadiene easily undergoes chemical aging under the condition of UV radiation and oxygen. Therefore, the mechanical properties of pure ABS and ABS composites containing 2.75 wt% KH-570 modified MDAPT@$BiVO_4$-700-60 were

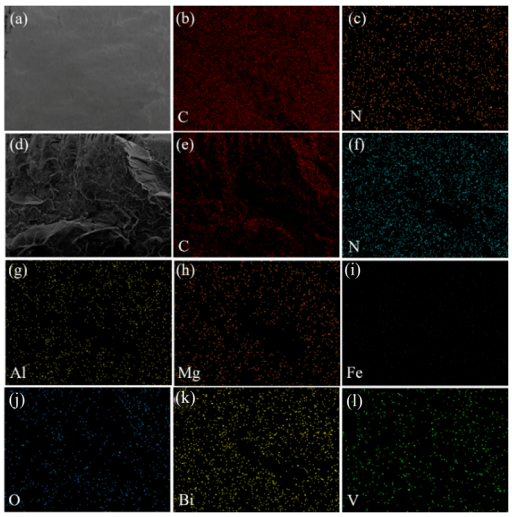

Fig. 8 Elemental mappings of the tensile splines of pure ABS (a–c) and ABS composites containing KH-570 modified MDAPT@$BiVO_4$-700-60 (d–l) after bending testing.

evaluated after being exposed to UV light for different times. It was clearly observed that the mechanical properties of pure ABS and ABS composites changed with the increase in the aging days.

As shown in Fig. 9a–c, the mechanical properties of pure ABS changed obviously with the increase in the aging time. The tensile strength of pure ABS presented an increasing trend with the prolonging in the aging days, but the elongation at break indicated a downtrend. The tensile strength of pure ABS increased from 53.49 MPa to 56.68 MPa after aging for 5 days under UV light, while the bending strength decreased from 76.54 MPa to 72.91 MPa. In the case of the ABS composites, the tensile strength decreased from 59.68 MPa to 57.04 MPa, and the bending strength decreased from 87.95 MPa to 82.92 MPa under UV light radiation for 5 days.

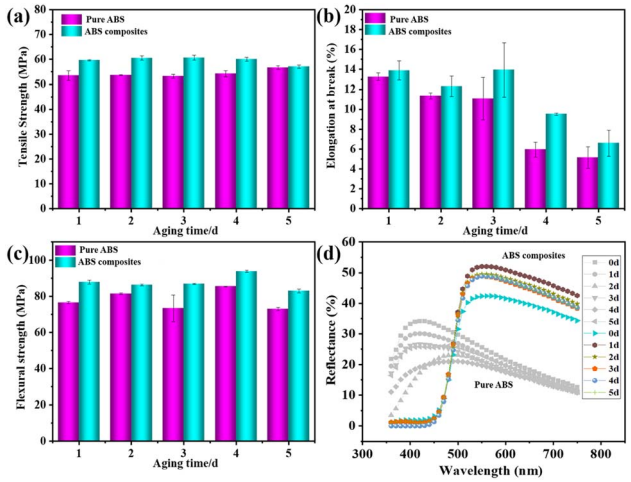

Fig. 9 (a–c) Effect of aging time on the mechanical properties of ABS and ABS composites. (d) UV-vis diffuse reflectance spectra of ABS and ABS composites.

Table 2 Effect of aging time on the colors of ABS composite containing 2.75 wt% KH-570 modified MDAPT @$BiVO_4$-700-60

	Color parameters of ABS composites					
Aging days	L^*	a^*	b^*	C^*	h^*	ASTM E313
0	71.84	−12.30	76.13	77.12	99.18	96.56
1	73.10	−12.49	75.05	76.08	99.45	95.22
2	73.64	−12.27	74.19	75.19	99.39	94.65
3	73.18	−12.18	76.72	77.68	99.02	96.50
4	72.03	−13.56	72.02	73.29	100.66	92.72
5	73.15	−12.45	75.42	76.44	99.38	95.46

Furthermore, the UV-vis diffuse reflectance spectra of ABS and ABS composites containing KH-570 modified MDAPT@$BiVO_4$-700-60 with the increase in the aging time are shown in Fig. 9d. It was obvious that the reflectance of ABS composites was higher than pure ABS, because MDAPT@$BiVO_4$-700-60 presented excellent dispersion properties in the ABS composites. According to UV-vis diffuse reflectance spectra, it was observed that hybrid pigments could absorb and reflect the visible light below 400 nm and above 500 nm (Fig. S4†), which suggested that hybrid pigments played important roles of absorption and reflection to UV and visible light, which might be in favor of enhancing the aging-resistance ABS.

After being exposed to outdoor sunny conditions for a period of time, ABS products usually become brittle and fade in color. It is thought that the aging of ABS is derived from the 1,4-butadiene component and the labile position of hydrogen atom in the α-position of the C=C bond, meaning it could be easily abstracted. As shown in Table 2, no obvious changes were observed for the b^* values of ABS composite before and after aging, which implied that there was almost no effect of the UV accelerated aging on the L^* and b^* values of the ABS composites. However, the L^* value of pure ABS splines obviously changed after aging (Table S3†), the L^* value of pure ABS deceases from 57.45 to 54.8 accompanied by an increase in the yellowness (b^*) after exposure to UV light. Therefore, the obtained hybrid pigments exhibited benign aging-resistance, presenting good application prospects in favor of enhancing the aging-resistance of ABS.

4. Conclusions

In summary, MDAPT@$BiVO_4$ hybrid pigments were successfully prepared with the assistance of twin-screw extrusion mechanochemistry. The results suggested that the mechanical force derived from screw extrusion effectively promoted the combination of Bi^{3+} and VO_4^{3-} on the MDAPT surface and the prepared hybrid pigments presented good color properties after incorporation of 60 wt% MDAPT. Compared with those of pure ABS, the tensile strength and bending strength of ABS composites containing 2.75 wt% hybrid pigments increased by 36.87% and 25.96%, respectively, which was attributed to the fact that KH-570 modification improved the surface/interfacial compatibility between pigments particles and ABS matrix. Furthermore, the incorporation of MDAPT@$BiVO_4$ hybrid

pigments also effectively enhanced the aging-resistance and thermal stability of ABS, resulting in the improvement of the long-term stability and service life of the polymer composites. Thus, this study presented great significance to realize the direct value-added and sustainable utilization of MDAPT and continuous cleaner preparation of $BiVO_4$ hybrid pigments.

Data availability

All data generated or analyzed during this study are included in the article and its ESI file.†

Author contributions

Lei Wu: methodology, visualization, writing – original draft. Bin Mu: conceptualization, writing – review and editing, supervision, project administration, funding acquisition. Hao Yang: methodology, visualization, writing – review and editing. Zhaoli Wang, Yongfeng Zhu, Hui Dou: validation, formal analysis. Aiqin Wang: conceptualization, writing – review and editing, supervision.

Conflicts of interest

The authors declare no conflicts of interest.

Acknowledgements

This work is supported by the Basic Research Creative Groups Project of the Science and Technology Plan of Gansu, China (23JRRA568), and the Young Scholar of Regional Development of the Chinese Academy of Sciences (The Science Development Talent Teach words [2022] No. 10).

References

1 R. P. Magisetty, D. Prajapati, R. Ambekar and B. Kandasubramanian, *J. Phys. Chem. C*, 2019, **123**, 28081–28092.
2 J. K. Kim, S. S. Kang, H. G. Kim and L. K. Kwac, *Polymers*, 2023, **15**, 863.
3 C. C. Kuo, N. Gurumurthy and S. H. Hunag, *Polymers*, 2023, **15**, 3424.
4 J. Wang, Y. C. Li, J. F. Song, M. Y. He, J. J. Song and K. Xia, *Polym. Degrad. Stab.*, 2015, **112**, 167–174.
5 E. Andersen, L. H. Bertelsen, M. Salomonsen, M. Kristensen, P. Kybelund, M. B. Sørensen and M. Hinge, *Polym. Degrad. Stab.*, 2020, **178**, 109183.
6 R. Fiorio, S. Villanueva Díez, A. Sánchez, D. R. D'hooge and L. Cardon, *Materials*, 2020, **13**, 212.
7 L. Wu, B. Mu, H. Yang, X. W. Wang and A. Q. Wang, *J. Appl. Polym. Sci.*, 2022, **139**, 52266.
8 Y. Y. Shi, Y. D. Hu, L. Zhang, Z. W. Wang, Q. H. Zhang, H. Cui, X. F. Zhu, J. Z. Wang, J. Chen and K. L. Wang, *Appl. Clay Sci.*, 2017, **137**, 249–258.
9 H. Yang, B. Mu, J. Xu, Y. J. Zhu and A. Q. Wang, *Ceram. Int.*, 2022, **48**, 27182–27191.
10 K. Linberg, P. C. Sander, F. Emmerling and A. A. L. Michalchuk, *RSC Mechanochem.*, 2014, **1**, 43–49.
11 A. Khazaei, L. Jafari-Ghalebabakhani, E. Ghaderi, M. Tavasoli and A. R. Moosavi-Zare, *Appl. Organomet. Chem.*, 2017, **31**, e3815.
12 M. Zayat and D. Levy, *Chem. Mater.*, 2000, **12**, 2763–2769.
13 X. W. Wang, A. J. Zhang, X. C. An and A. Q. Wang, *Powder Technol.*, 2019, **343**, 68–78.
14 R. R. A. Bolt, J. A. Leitch, A. C. Jones, W. I. Nicholson and D. L. Browne, *Chem. Soc. Rev.*, 2022, **51**, 4243–4260.
15 T. Shi, Y. M. Liu, Y. L. Zhang, Y. J. Lan, Q. F. Zhao, Y. J. Zhang and ang H. B Wang, *Int. J. Concr. Struct. Mater.*, 2022, **16**, 1–10.
16 Y. S. Lu, W. K. Dong, W. B. Wang, Q. Wang, A. P. Hui and A. Q. Wang, *Appl. Clay Sci.*, 2019, **167**, 50–59.
17 H. Zhang, W. B. Wang, X. W. Wang, J. Xu, Y. S. Lu and A. Q. Wang, *Powder Technol.*, 2022, **396**, 456–466.
18 X. W. Wang, B. Mu, A. P. Hui, Q. Wang and A. Q. Wang, *Dyes Pigm.*, 2018, **149**, 521–530.
19 W. C. Yan, D. Liu, D. Y. Tan, Y. P. Yuan and M. Chen, *Spectrochim. Acta, Part A*, 2012, **97**, 1052–1057.
20 X. Y. Li, Y. Jiang, X. Q. Liu, L. Y. Sho, D. Y. Zhang and L. B. Sun, *ACS Sustainable Chem. Eng.*, 2017, **5**, 6124–6130.
21 M. F. R. Samsudin, S. Sufian, R. Bashiri, N. M. Mohamed and R. M. Ramli, *J. Taiwan Inst. Chem. Eng.*, 2017, **81**, 305–315.
22 X. Wang, Y. Shen, G. Zuo, F. Li, Y. Meng and L. Hou, *Mater. Res. Innovations*, 2016, **20**, 500–503.
23 M. Barczewski, D. Matykiewicz and B. Hoffmann, *Int. J. Polym. Sci.*, 2017, 7043297.
24 L. Pang, N. C. Paxton, J. Y. Ren, F. Liu, H. F. Zhan, M. A. Woodruff, A. Bo and Y. T. Gu, *ACS Appl. Mater. Interfaces*, 2020, **12**, 47993–48006.
25 S. Khandelwal and K. Y. Rhee, *Composites, Part B*, 2020, **192**, 108011.
26 P. Singh and A. K. Ghosh, *Mater. Des.*, 2014, **55**, 137–145.
27 T. Nazari, H. Garmabi and A. Arefazar, *J. Appl. Polym. Sci.*, 2012, **126**, 1637–1649.
28 X. W. Wang, B. Mu, Z. Zhang and A. Q. Wang, *Composites, Part B*, 2019, **174**, 107035.
29 J. Xu, L. Wu, B. Mu, Y. S. Lu, Q. Wang and A. Q. Wang, *Appl. Clay Sci.*, 2024, **258**, 107492.
30 M. R. Rahman, J. L. C. Hui and S. B. Hamdan, 1 - Introduction and reinforcing potential of silica and various clay dispersed nanocomposites, in *Silica and Clay Dispersed Polymer Nanocomposites*, ed. M. R. Rahman, Woodhead Publishing, 2018, pp. 1–24.
31 R. M. Santos, G. L. Botelho and A. V. Machado, *J. Appl. Polym. Sci.*, 2010, **116**, 2005–2014.
32 L. Wang, B. Shi, E. Z. Hu, K. H. Hu and X. G. Hu, *Tribol. Int.*, 2019, **131**, 415–423.